Molecular Cell, Vol. 10, 259–269, August, 2002, Copyright ©2002 by Cell Press

Proteases Acting on Mutant Huntingtin Generate Cleaved Products that Differentially Build Up Cytoplasmic and Nuclear Inclusions

Astrid Lunkes,[1,3,4] Katrin S. Lindenberg,[2] Léa Ben-Haïem,[1] Chantal Weber,[1] Didier Devys,[1] G. Bernhard Landwehrmeyer,[2] Jean-Louis Mandel,[1] and Yvon Trottier[1,3]

[1]Institut de Génétique
et de Biologie Moléculaire et Cellulaire
CNRS/INSERM/ULP
B.P.163
67404 Illkirch Cédex
CU de Strasbourg
France

[2]Department of Neurology
University of Ulm
89075 Ulm
Germany

Summary

Proteolytic processing of mutant huntingtin (mhtt) is regarded as a key event in the pathogenesis of Huntington's disease (HD). Mhtt fragments containing a polyglutamine expansion form intracellular inclusions and are more cytotoxic than full-length mhtt. Here, we report that two distinct mhtt fragments, termed cp-A and cp-B, differentially build up nuclear and cytoplasmic inclusions in HD brain and in a cellular model for HD. Cp-A is released by cleavage of htt in a 10 amino acid domain and is the major fragment that aggregates in the nucleus. Furthermore, we provide evidence that cp-A and cp-B are most likely generated by aspartic endopeptidases acting in concert with the proteasome to ensure the normal turnover of htt. These proteolytic processes are thus potential targets for therapeutic intervention in HD.

Introduction

Huntington's disease (HD) is the most frequent of a group of nine inherited neurodegenerative disorders caused by expansion of a CAG trinucleotide repeat encoding polyglutamine (polyGln) (Nakamura et al., 2001; Zoghbi and Orr, 2000). Several observations indicate that the polyGln-expanded proteins adopt a novel conformation, which renders them prone to aggregate and conveys toxic properties within a distinct cellular context (Lunkes et al., 1999; Perutz et al., 1994; Scherzinger et al., 1997; Trottier et al., 1995b). Inclusions within the cytoplasm or within the nucleus of neurons are therefore a pathological hallmark of these disorders, both in patient brains and in model systems (Davies et al., 1997; Di Figlia et al., 1997; Scherzinger et al., 1997).

Inclusions in brains of HD patients (Di Figlia et al., 1997) and of a knockin mouse model (Wheeler et al., 2000) were shown to be primarily composed of short truncated derivatives of mhtt, raising the possibility that proteolytic cleavage of htt plays a key role in pathogenesis. Several other observations support this hypothesis. First, the expression of a truncated mhtt fragment corresponding to exon 1 was sufficient to cause a pathological phenotype in mouse models that is more severe than that elicited by the full-length mhtt (Davies et al., 1997; Yamamoto et al., 2000). Second, cellular models showed that the length of expressed mhtt correlates inversely with its potential to aggregate and to cause cell death (Hackam et al., 1998; Lunkes and Mandel, 1998). Finally, short mhtt fragments, but not the full-length protein, are enriched in the nucleus (Hackam et al., 1998; Lunkes and Mandel, 1998). Along the same line, evidence for proteolytic cleavage of htt was reported both from in vitro and in vivo studies (Di Figlia et al., 1997; Wellington et al., 2000; Kim et al., 2001; Mende-Mueller et al., 2001; Wheeler et al., 2000). However, up to now, no in-depth analysis has been performed of the upstream processes underlying the formation of inclusions in vivo. Based on the potential importance of this cleavage product in the pathology of the disease, a characterization of the sites involved in the cleavage process could provide new targets for therapeutic interventions.

Aggregated mutant proteins forming nuclear inclusions (NI) were thought to cause cellular dysfunction in polyGln disorders, since NIs are detectable prior to onset of symptoms in HD mouse models and in human brain (Davies et al., 1997; Gutekunst et al., 1999). More recent findings, however, suggested that the presence of soluble mutant protein is sufficient to initiate the pathology (Hodgson et al., 1999; Klement et al., 1998), while at later stages, formation of NIs may aggravate neuronal dysfunction and cause cell death. Support for the latter hypothesis comes from several groups who demonstrated that proteins essential for cellular survival are trapped in NIs (Steffan et al., 2000; Suhr et al., 2001). Although the mechanisms whereby expanded Gln repeats induce cell dysfunction are not completely understood, the presence of the expanded polyGln in the nucleus seems to be required for pathogenesis.

Recently, we developed an inducible neuronal cell model for HD in which the formation of NIs in cells expressing full-length mhtt is observed in a time-dependent manner (Lunkes and Mandel, 1998), contrasting with many cellular models in which NIs are seen only when truncated htt forms are expressed (Lunkes and Mandel, 2000). In our model, NIs were ubiquitinated and contained N-terminal mhtt fragment smaller than the one generated by caspase activity (Wellington et al., 2000), thus appearing very similar to the aggregated htt breakdown product observed in brains of HD patients (Di Figlia et al., 1997). This suggested that processing steps generating fragments with high aggregation potential operate in our cellular model, possibly in a manner similar to the one in patient brains.

In the present study, we focused on the characterization of the mhtt fragments building up the inclusions and the proteolytic activities generating these fragments.

[3]Correspondence: yvon@igbmc.u-strasbg.fr (Y.T.), astrid.lunkes@embo.org (A.L.)

[4]Present address: European Molecular Biology Organization, Meyerhofstrasse 1, 69117 Heidelberg, Germany.

Using a panel of anti-htt antibodies in immunofluorescence (IF) analysis, we show that in htt-expressing cells and also in HD brain, NIs and cytoplasmic inclusions (CIs) are made up of N-terminal htt fragments differing in length. Three independent methods were employed to characterize the cleavage domains in htt and to identify a unique N-terminal fragment building up NIs. Finally, we provide evidence that clearance of htt is ensured by a multistep proteolysis that involves aspartic proteases and the proteasome and that during this process, N-terminal mhtt fragments with high aggregation potential are generated.

Results

Characterization of Cytoplasmic and Nuclear Inclusions in a Cellular Model of HD

Using a panel of monoclonal (mAb) and polyclonal antibodies (pAb) recognizing htt epitopes between aa 1 and aa 500 (Figure 1A), we performed single or double IF studies to characterize mhtt fragment(s) making up CIs and NIs in differentiated neuronal cells expressing Flag-tagged full-length mhtt (FL-hd116) or truncated versions of mhtt (T-hd73 or T-hd122) (see Figure 1 and Lunkes and Mandel, 1998). In cells expressing FL-hd116, NIs reacted readily with the anti-Flag mAb M2 and with two htt-specific Abs, pAb 1259 and mAb 2B4, which recognize epitopes close to the polyGln domain (Figure 1B, and data not shown). In double IF, all NIs were stained with M2 and 1259, indicating that no cleavage occurs N-terminal to the polyGln stretch (data not shown). In contrast, in double IF experiments using one of these three reference Abs (M2, 1259, or 2B4) in combination with an Ab recognizing more C-terminal epitopes on htt such as mAb 1H6, pAb 214, and mAb 4C8, no costaining of NIs was observed (Figure 1B, first and second rows, and Lunkes and Mandel, 1998). A similar pattern of NI immunoreactivity was seen in cells expressing T-hd122 or T-hd73, demonstrating that this htt derivative is proteolysed similarly to FL-hd116, as observed at 6–14 days (data not shown). Taken together, these results indicate that htt is cleaved N-terminal to the epitope of mAb 1H6 and C-terminal to the epitopes of Abs 2B4 or 1259. We then mapped the epitope of mAb 1H6 to the region of aa 115–129 (data not shown), thereby defining the protease-susceptible domain between the polyGln stretch (aa 40) and aa 115–129.

To overcome the lack of suitable antibodies directed to this domain, we generated the construct T-hd73-HA in which an HA-tag epitope was introduced at position aa 82 of htt (Figure 1A). We first confirmed in a double IF experiment that NIs formed in differentiated cells expressing T-hd73-HA were costained with pAb 1259 and an anti-HA mAb (Figure 1B, fourth row). In contrast, when using mAb 1H6 and an anti-HA pAb in double IF, we observed that the anti-HA pAb labeled NIs, while mAb 1H6 detected htt only in the cytoplasm (Figure 1B, fifth row). This result indicates cleavage between the epitopes of Abs HA and 1H6, narrowing the site of cleavage down to a domain between aa 82 and aa 115–129. We designated the N-terminal htt fragment prone to form nuclear aggregates cleavage product A (cp-A).

Next, to analyze the immunoreactivity of CIs, we used differentiated cells expressing T-hd122 instead of FL-hd116, as the frequency of aggregates is higher with truncated forms (Lunkes and Mandel, 1998). Among the CIs visualized by Abs 1259 or M2, 93% were positive with mAb 1H6, while only 57% were stained with pAb 214, whose epitope is located more C-terminal (Table 1 and Figure 1B, third row). Some CIs were also labeled with mAb 4C8, which detects an even more C-terminal epitope (data not shown). Immunoelectron microscopy performed with mAb M2 and peroxidase/DAB labeling confirmed that CIs have granular and filamentous electron-dense features (see Supplemental Figure S1 at http://www.molecule.org/cgi/content/full/10/2/259/DC1) commonly seen for aggregated polyGln proteins (Davies et al., 1997). Our results indicate that fragments making up CIs are derived from at least two different cleavage events: one event cleaving off the epitope of mAb 1H6 and generating a fragment with the same antigenic properties as cp-A, and a second event that cleaves between the epitopes of Abs 1H6 and 214, generating a larger fragment that we designated cp-B. Thus, from these findings, we conclude that NIs and CIs generated in our cellular model differ with respect to the nature of htt fragments they contain.

Immunohistochemical Characterization of Cytoplasmic and Nuclear Inclusions in HD Brain

To examine whether the differential make-up of NIs and CIs seen in the cellular model is also observed in HD brain, we used the same set of Abs in immunohistochemical (IHC) studies on human frontal cortices of six HD patients (four grade 4 and two grade 3 brains) and three controls. When we employed a single labeling method involving the avidin-biotin-peroxidase complex and DAB, cytoplasmic neuronal labeling was seen with Abs 1259, 2B4, 1H6, 214, and 4C8 in both control and HD brains (see Supplemental Figure S2 and Supplemental Table S1 at http://www.molecule.org/cgi/content/full/10/2/259/DC1). Moreover, Abs 1259 and 2B4 densely stained NIs in all HD cortices, as well as neuronal CIs.

In double IF studies, a very similar staining pattern was seen with Abs 1259 and 2B4, with no discrepancies in the detection of inclusions (data not shown). However, when pAb 1259 or mAb 2B4 were used in combination with mAb 1H6, pAb 214, or mAb 4C8, none of the Abs detecting more C-terminal epitopes labeled NIs (Figure 2, first, third, and fourth rows), whereas some 1259-positive CIs were costained with mAb 1H6 (Figure 2, second row). We thus conclude that NIs of HD brain are composed of htt fragments proteolysed N-terminal to the epitope of mAb 1H6. The composition of CIs, in contrast, is heterogeneous, with some CIs bearing the epitope of mAb 1H6 and some not. These in situ observations on HD brains are in agreement with the data obtained in mhtt-expressing cells and thus validate the cellular model as a tool to identify the proteolytic cleavage sites relevant in HD.

Biochemical Characterization of Disaggregated Nuclear Inclusions

Previous studies showed that the aggregates formed by mhtt in vitro and in vivo are insoluble in regular protein

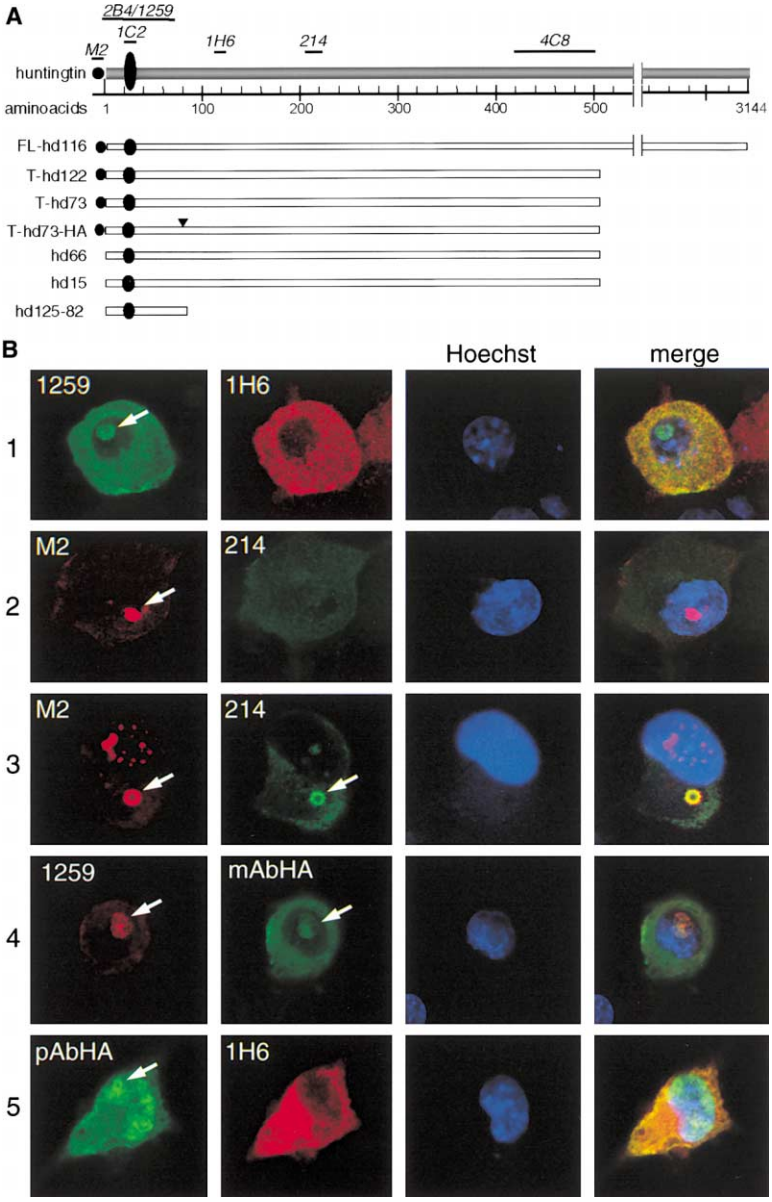

Figure 1. Antigenic Properties of Nuclear and Cytoplasmic Inclusions Formed in a Cellular Model of HD

(A) Scheme showing huntingtin constructs (white boxes) and map of anti-htt antibodies (italic) along the wild-type htt amino acid sequence (with 21 CAG-coding Gln repeats). FL-hd116, T-hd122, and T-hd73 were Flag-tagged (small closed circle) cDNA constructs under a doxicycline inducible promoter (previously described in Lunkes and Mandel, 1998), and encoded, respectively, full-length htt with 116 Glns, and truncated versions of htt (ending at position aa 502) with 122 and 73 Glns. T-hd73-HA had an HA-tag sequence (closed triangle) introduced at position aa 82 in T-hd73. hd125-82 (125 Glns), hd66 (66 Glns), and hd15 (15 Glns) constructs encoded truncated versions of htt (ending at aa82 and aa 502) under a SV40 promoter. 1259 polysera and mAb 2B4 recognize htt aa 1–82; mAb 1H6, aa 115–129; mAb 4C8, aa 414–503 (Trottier et al., 1995a); 214 polysera, aa 214–229. For each Ab, specificity versus background staining was verified on control and transfected cells. The polyGln stretch is represented by a black ellipse symbol.

(B) Confocal images of NG108 cells expressing mutant htt illustrate cleavage events. In FL-hd116 cells (rows 1–3), NIs (rows 1 and 2, arrows) react only with Abs recognizing very N-terminal epitopes such as pAb 1259 and anti-Flag M2 mAb, while mAb 1H6 and pAb 214 lack immunoreactivity on NIs. In contrast, mAb 1H6 and in some instances pAb 214 are able to detect CIs (row 3, arrow; and see Table 1). In cells expressing T-hd73-HA (rows 4 and 5), NIs (arrows) are detected with pAb 1259 and with the anti-HA mAb or pAb (which also reveals diffuse nuclear staining as background), while mAb 1H6 displays only cytoplasmic reactivity (row 5).

lysis buffer (SDS-buffer) (Scherzinger et al., 1997), precluding their biochemical analysis by SDS-PAGE. In an attempt to analyze the htt content of NIs, we used T-hd122-expressing cells differentiated for 13 days to generate NIs at high frequency (Lunkes and Mandel, 1998). We isolated the respective cytoplasmic and nuclear SDS-soluble material (Figure 3A), which were then solubilized (disaggregated) with formic acid (FA) and analyzed by Western blot (WB) using mAb 1C2, which recognizes specifically expanded polyGln stretches (Trottier et al., 1995b). While the expressed T-hd122 protein of 110 kDa was mainly observed in the SDS-soluble cytoplasmic fraction and to a lesser extent in the nuclear fraction, multiple immunoreactive bands were detected in the SDS-resistant (FA-soluble) nuclear fraction, with the lowest molecular weight (MW) band at 55 kDa (Figure 3B) the most prominent one. The presence of the T-hd122 protein in the nuclear extracts was unexpected, since no nuclear immunoreactivity was seen with mAb 4C8 in IF analysis. Given that we and others (Kegel et al., 2000) detected truncated mhtt in the perinu-

Table 1. Cytoplasmic Inclusions Are Composed of Htt Fragments Differing in Length

Total number of cells	Percentage of Cells Detected with Ab			
	Anti-Flag	1259	1H6	214
267	100	–	–	57 ± 7
299	–	100	93 ± 5	–

NG108 cells expressing T-hd122 were evaluated after 6 days of differentiation by double immunofluorescence with either Ab combination anti-Flag/214 or 1259/1H6. Since Abs anti-Flag and 1259 detect cytoplasmic inclusions equally well, they were used for normalization. The result represents the mean of three independent experiments with standard deviation.

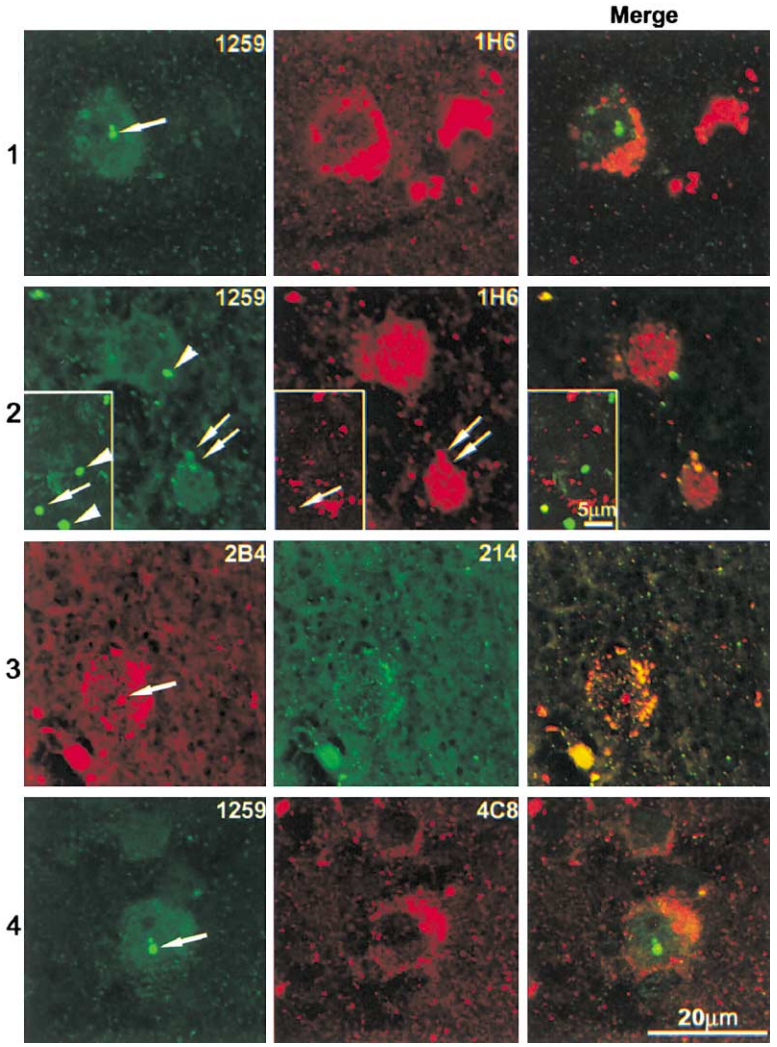

Figure 2. Make-up of Nuclear and Cytoplasmic Inclusions in HD-Brain

Confocal images of double IF on HD brain tissue display antigenic properties of NIs and CIs. NIs were stained by Abs 1259 and 2B4 (rows 1, 3, and 4, arrows) but not by Abs recognizing more C-terminal epitopes, 1H6 (row 1), 214 (row 3), and 4C8 (row 4), suggesting that a cleavage event occurs between the epitopes of Abs 1259 and 1H6. In contrast, a subset of 1259-labeled CIs (row 2, arrows) were costained with mAb 1H6 while other CIs were exclusively immunopositive for pAb 1259 (row 2, arrowheads). The inset in row 2 shows a chain of CIs within the neuropil.

clear area in some cells, it is likely that this localization might give rise to a slight nuclear contamination during subcelluar fractionation (estimated level of nuclear T-hd122 was <10%). Alternatively, the amount of T-hd122 per individual nucleus might be too low to be revealed by IF.

To confirm that the lowest band at 55 kDa corresponds to cp-A identified by IF, we tested its antigenic properties using the panel of anti-htt Abs (Figure 3C). All Abs detected T-hd122 with equal intensity in the nuclear SDS-soluble fraction. In contrast, the 55 kDa band of the FA-soluble fraction was only visualized with mAbs 1C2 and 2B4, indicating that it displays the same antigenic properties as cp-A. It is unlikely that this 55 kDa htt fragment is derived from chemical cleavage during the experimental procedure, since no cleavage sites are predicted for formic acid in the first 545 aa of htt. Moreover, it is noteworthy that the bands at a MW higher than the one at 55 kDa were also detected with mAb 1C2 and less strongly by mAb 2B4 (data not shown), but not with Abs recognizing more C-terminal epitopes. Since NIs in our cellular model (Lunkes and Mandel, 1998) and in HD brain (Di Figlia et al., 1997) are ubiquitinated, we reasoned that these high MW bands may represent polyubiquitinated derivatives of the 55 kDa cp-A. Indeed, the anti-ubiquitin Ab detected the same high MW bands as mAb 1C2 (Figure 3D), with an intensity that increases with their respective size, suggestive of polyubiquitination. Taken together, the biochemical results are consistent with the IF analysis and indicate that NIs are composed of the 55 kDa cp-A and, most likely, its polyubiquitinated derivatives.

Applying the same disaggregation protocol to brain homogenate, we observed an intense 1C2-labeled smear of mhtt (ranging from 60 kDa to very high MW) in HD brain that was not seen in control brain (see Supplemental Figure S3 at http://www.molecule.org/cgi/content/full/10/2/259/DC1). Immunoprobing with anti-ubiquitin Ab indicated that FA-soluble material from HD and control brains was largely composed of ubiquitinated proteins, suggesting that the aggregated mhtt fragments in HD brains are entirely ubiquitinated, thereby precluding further analysis of their size and antigenic property.

Proteolytic Activities Acting on Huntingtin

We next attempted to determine which proteolytic activities generate htt fragments cp-A and cp-B. The protea-

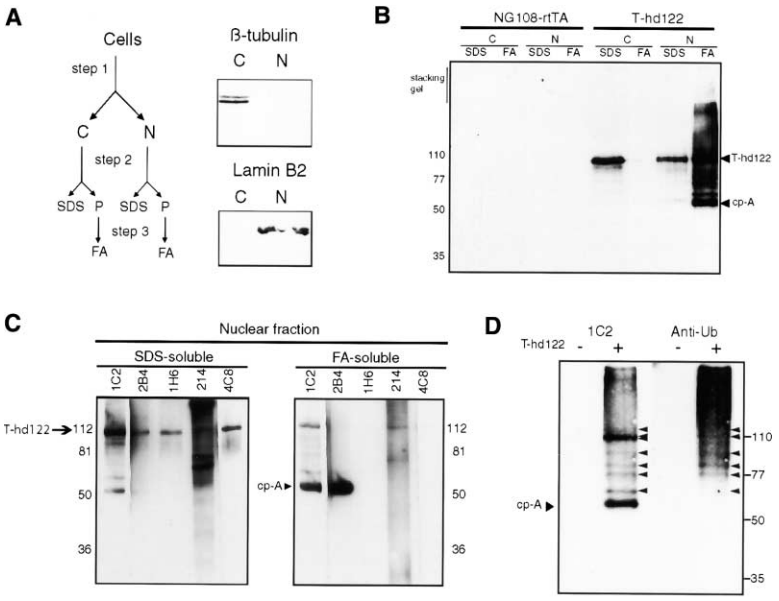

Figure 3. Disaggregation of Nuclear Inclusions

(A) A three-step protocol was used to fractionate and dissociate aggregated mhtt fragments. In step 1, differentiated cells were first fractionated to enrich for cytoplasmic (C) and nuclear (N) proteins, as revealed by the presence of β-tubulin and lamin B2 in the corresponding fractions (50 μg of protein), respectively. In step 2, C and N protein fractions were solubilized using SDS buffer and centrifuged to generate a supernatant containing SDS-soluble protein fractions (SDS) and a pellet (P) of SDS-resistant proteins. The latter were dissociated in step 3 using formic acid (FA) prior to WB analysis.

(B) WB analysis of the four fractions obtained from NG108-rtTA parental cells and T-hd122-expressing cells differentiated for 13 days. While Ab 1C2 detected T-hd122-expressed protein in the soluble fraction of cytoplasm and nucleus, a smear containing a predominant band of 55 kDa is observed in the SDS-resistant (FA-soluble) nuclear fraction. No cross-reacting material is found in fractions of the parental cell line. Fifty micrograms of SDS-soluble extracts from C and N, and 1/5 of the respective FA-soluble fractions were loaded on SDS-PAGE.

(C) The 55 kDa fragment has the same antigenic properties as fragment cp-A. While all Abs tested detected the T-hd122 form with similar signal intensities in the soluble nuclear fraction (left blot), the 55 kDa fragment enriched in the FA-soluble fraction is only detected by Abs 1C2 and 2B4, but not by Abs 1H6, 214, or 4C8. The two blots shown were exposed for the same period of time. Longer exposure of the right blot revealed a faint T-hd122 band with all Abs. The 65 kDa band revealed with pAb 214 is due to cross-reaction, since it is also observed in untransfected cells.

(D) Aggregated 55 kDa cp-A is partially ubiquitinated. In the SDS-resistant (FA-soluble) nuclear fraction of T-hd122-expressing cells, an Ab directed against ubiquitin reveals bands at higher MW than the 55 kDa cp-A, similar to those detected by Ab 1C2. No polyGln- or ubiquitin-containing material is detected in the SDS-resistant fraction of control cells.

some is one of the most important degradation machineries of the cell and therefore a possible candidate to generate truncated versions of ubiquitinated proteins due to partial proteolysis. Alternatively, given that htt is a very large protein (350 kDa), other protease(s) might act on htt before it enters the core of the proteasome to reduce the size of htt polypeptides that have to be unfolded and degraded. To discriminate between the two scenarios, we examined the role of the ubiquitin/proteasome pathway in the normal clearance of htt. We coexpressed his-tagged ubiquitin together with htt of 502 aa with 15 or 66 Gln (hd15 and hd66, Figure 1A) or an even shorter htt fragment comprising the first 82 aa (hd125-82) and recovered ubiquitinated htt by affinity purification on a Nickel column, confirming that soluble mutant and wild-type htt undergo ubiquitination (see Supplemental Figure S4 at http://www.molecule.org/cgi/content/full/10/2/259/DC1). We then tested whether inhibitors of the proteasome interfered with the normal clearance of htt. When hd15-expressing COS cells were treated with proteasome inhibitor ALLN, mAb 4C8 revealed several bands slightly higher in MW than hd15, indicative of ubiquitination (Figure 4A). Interestingly, when the same extracts were analyzed with mAb 2B4, detecting an N-terminal htt epitope, two distinct low MW bands (23 and 30 kDa) were detected. Similarly, two htt breakdown products were readily detected by mAb 1C2 in ALLN treated, undifferentiated NG108 cells expressing T-hd73 or T-hd122 or, most importantly, full-length mhtt FL-hd116 (Figure 4B). The notable increase in their MW correlates with the size of polyGln expansion. As these distinct breakdown products were also generated in cells treated with other proteasome inhibitors, such as lactacystin or MG132 (data not shown), but not or only very faintly in DMSO treated samples or in cells exposed to control inhibitor ALLM, this suggests that a protease acts on htt before its normal clearance by the proteasome.

Given that treatment with proteasome inhibitors led to an increased frequency of inclusions in htt-expressing cells (data not shown, Jana et al., 2001), we hypothesized that these htt breakdown products may correspond to accumulating cp-A and cp-B, respectively. In agreement with this hypothesis, we detected these htt breakdown products in the FA-soluble fraction of T-hd122-expressing cells treated with ALLN (Figure 4C). In addition, the htt products seen under proteasome inhibition have the same antigenic properties as cp-A and cp-B (Figure 4C), with the shortest one being detected with Abs 1C2 and 2B4, but not with mAb 1H6, and the larger one reacting with all three Abs. Finally, we confirmed that the shorter product observed in ALLN-treated cells is equivalent in size to cp-A, which builds up NIs in cells expressing T-hd122 for 13 days (Figure 4D). Thus, we suggest that inhibition of the proteasome provokes a dramatic increase in the level of soluble cp-A and cp-B, which within a few hours build up inclusions, a process otherwise requiring up to 18 days in differentiated NG108 cells expressing htt.

To identify the family of proteases releasing cp-A and cp-B, homogenates of T-hd73-expressing cells were subjected to self-digestion at 37°C for 1 hr and then

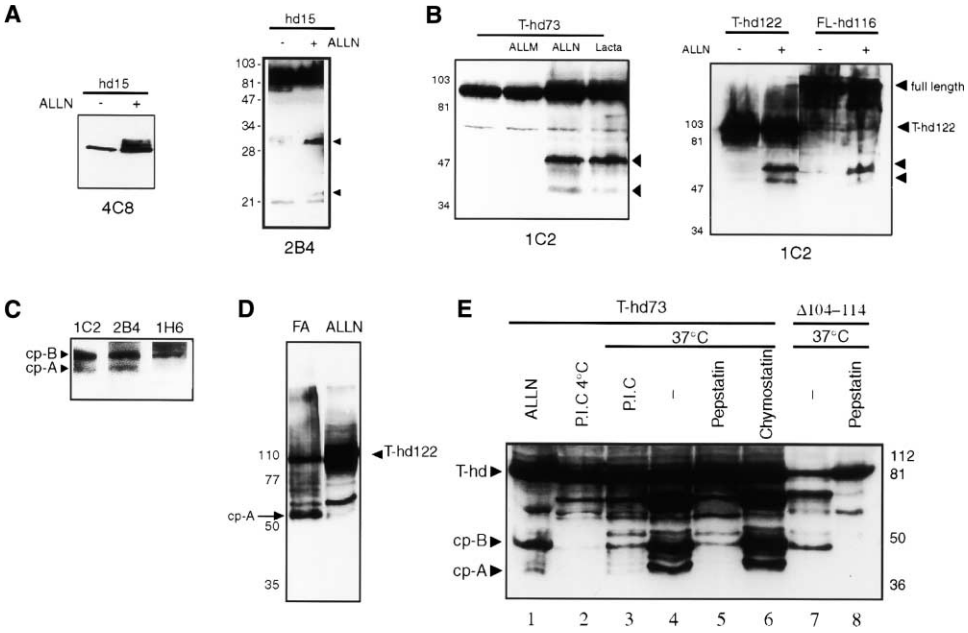

Figure 4. Proteolytic Activities Acting on Huntingtin

(A and B) Proteasome inhibition leads to accumulation of ubiquitinated htt and N-terminal htt breakdown products. (A) Protein extracts (50 μg) from HD15-expressing COS cells treated for 6 hr with proteasome inhibitor ALLN (+) or the solvent DMSO (−) were analyzed on WB. Under proteasome inhibition, mAb 4C8 detects multiubiquitinated forms of hd15 (left panel). MAb 2B4, in addition, reveals two N-terminal htt breakdown products (arrowheads) that are not seen in control cells. (B) Similarly, in undifferentiated NG108 cells expressing T-hd73, T-hd122, or FL-hd116 (for 48h), mAb 1C2 reveals two htt breakdown products (unlabeled arrowheads) in samples treated with proteasome inhibitors (ALLN or lactacystin), but not in those incubated with a control inhibitor (ALLM) or the solvent only. The sizes of the breakdown products in the respective panels increase with length of the polyGln stretch of the expressed htt construct.

(C) Antigenic properties of the low molecular weight htt fragments seen under proteasome inhibition correspond to those of cp-A and cp-B. T-hd122-expressing cells were treated with ALLN, and the proteins of the FA-soluble fraction were analyzed on WB using Abs 1C2, 2B4, and 1H6. While cp-A immunoreacted only with Abs 1C2 and 2B4, cp-B is, in addition, detected with mAb 1H6.

(D) The shortest htt fragment seen under proteasome inhibition has the same size as cp-A. Sizes of htt fragments obtained after ALLN treatment were compared to the one of the FA-solubilized cp-A generated from T-hd122 cells after 13 days of culture. The WB was immunoprobed with Ab 1C2.

(E) Aspartic protease activities generate cp-A and cp-B in an in vitro self-digestion assay. Protein homogenates (40 μg) of undifferentiated NG108 cells expressing T-hd73 (lanes 2–6) or Δ104-114 (lanes 7 and 8) were incubated for 1 hr at the indicated temperature in the absence of inhibitors (−), in the presence of a protease inhibitor cocktail (P.I.C.), or in the presence of pepstatin or chymostatin alone. The incubated samples together with an extract of T-hd73 cells treated with ALLN (lane 1) were analyzed on WB using mAb 1C2. In the absence of inhibitors, self-digested T-hd73 cell extract (lane 4) released fragments cp-A and cp-B (and another fragment at 70 kDa). This in vitro htt proteolysis was specifically blocked by P.I.C. or pepstatin, but not by other individual inhibitors (lane 6, and data not shown). Self-digested Δ104-114 extract did not generate fragment cp-A (even after longer exposure of the blot), whereas cp-B was produced in the absence of pepstatin, but not in its presence.

analyzed on WB using mAb 1C2 (Figure 4E, lanes 2–6). Self-digestion treatment without protease inhibitors generated major htt fragments similar in size to cp-A and cp-B. In contrast, htt proteolysis was prevented in the presence of a protease inhibitor cocktail (P.I.C.) (containing aprotinin, antipain, chymostatin, leupeptin, and pepstatin). When these inhibitors were used individually, only pepstatin, an inhibitor of aspartic endopeptidases, blocked htt proteolysis (Figure 4E, and data not shown). Thus, these results suggest that the protease(s) generating cp-A and cp-B in NG108 cells belong to the family of aspartic endopeptidases.

Cleavage Site/Domain Releasing Cp-A and Specificities of the Protease Involved

Several independent results indicate that htt cleavage product cp-A accumulates in our cellular model and builds up NIs. To define the site where cleavage occurs to release cp-A (designated as site A), we pursued four approaches for which we generated several htt versions with C-terminal truncations, internal deletions, or double amino acid substitutions (Figure 5A). Our previous IF study (Figure 1B) indicated that site A lies between aa 82 and aa 115–129. To locate it more precisely, we used in a first approach truncated mhtt versions of 101 aa and 124 aa (designated hd73-101aa and hd73-124aa in Figure 5A) as size standards to map the size of cp-A produced in ALLN-treated htt-expressing cells. Figure 5B shows that cp-A (lanes 3 and 5) migrated between hd73-101aa and hd73-124aa (lanes 1 and 2), indicating that site A is located between aa 101 and 124. The second approach relied on the use of deleted htt constructs in the proteasome inhibition assay. Among the expressed constructs carrying a deletion in the identified domain (Figure 5B, lanes 6 and 7; and data not shown), Δ104-114aa was the only one that did not produce cp-A. It is noteworthy that cells expressing htt proteins in which the internal deletions are placed further

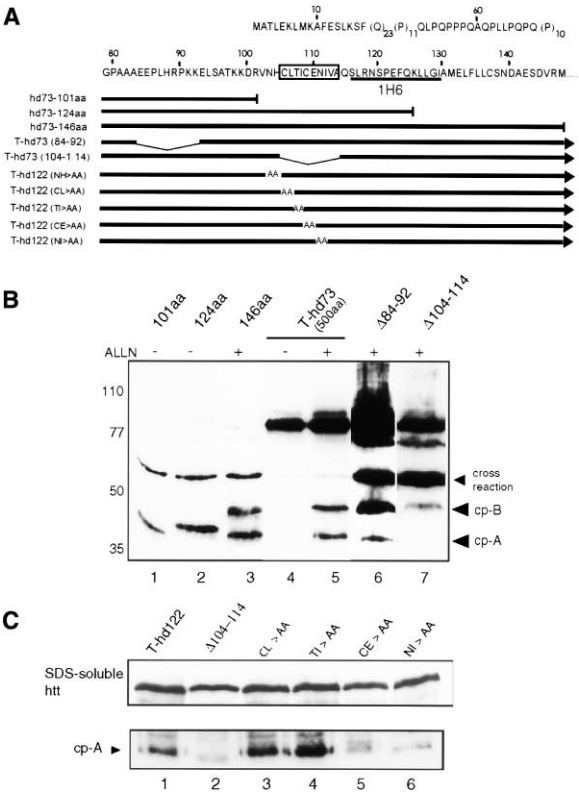

Figure 5. Determination of the Domain Releasing Cp-A

(A) Huntingtin constructs were designed to have C-terminal truncations, internal deletions, or amino acid substitutions, in order to identify cleavage site A. The N-terminal part of the wild-type htt amino acid sequence is shown on the top, together with the 1H6 epitope (underlined) and the 10 aa protease-susceptible domain that is cleaved to release cp-A. All constructs contain the first 502 aa of htt, except for hd73-101aa, hd73-124aa, and hd73-146aa, which carry an HA-tag, (11 aa) at their C terminus, therefore resulting in 90aa-HA, 113aa-HA, and 135aa-HA.

(B) Cells expressing different truncated versions of htt and deletion constructs were subjected to proteasome inhibition treatment. The protein extracts were investigated on a WB using Ab 1C2. The cp-A fragment produced in hd73-146aa and T-hd73 (502 aa) treated with ALLN (lanes 3 and 5, respectively) migrates on SDS-PAGE between hd73-101aa (lane 1) and hd73-124aa (lane 2), indicating that cleavage occurs between aa 101 and 124. Among several deletion constructs analyzed (lanes 6 and 7, and data not shown), Δ104-114 is the one that does not release fragment cp-A under proteasome inhibition conditions. The 60 kDa band (and the 77 kDa band in lanes 6 and 7) was also observed in protein extract of nontransfected cells and was due to a protein cross-reacting with a given antibody preparation of mAb 1C2 (data not shown).

(C) Cp-A production in cells expressing deletion and substitution mutants. Differentiated cells expressing T-hd122 or the mutants for 18 days were harvested, and SDS-resistant proteins were solubilized with FA and analyzed on WB using mAb 1C2. The upper panel shows the expression level of the htt constructs in SDS-soluble extract (50 μg of protein). In the lower panel, levels of cp-A released from T-hd122, T-hd122Δ104-114, and substitution mutants are compared.

upstream (Δ84-92 or Δ93-101aa) or downstream (Δ114-123aa) of aa 104–114 still generated cp-A (Figure 5B, and data not shown), although to a somewhat reduced level, suggesting that the tertiary structure of the region is important for cleavage. In addition, similar results were obtained in the in vitro self-digestion assay, in which the deletion of aa 104–114 also prevented the release of cp-A (Figure 4E, lanes 7 and 8). Based on these results, we located the domain containing cleavage site A between aa 104 and 114.

In a third approach, the effect of Δ104-114aa on the release of cp-A was analyzed in the context of differentiated NG108 cells maintained in culture for 18 days, an experimental condition better representing the physiological setting. While cp-A was revealed in FA-soluble extracts of cells expressing T-hd122, no such fragment was detected by mAb 1C2 in htt deleted for aa 104–114 (Figure 5C, lower panel), despite similar expression levels of both constructs in SDS-soluble extract (Figure 5C, upper panel, lanes 1 and 2, respectively). Instead, mAb 1C2 detected a faint fragment slightly shorter than cp-A. This shorter fragment was able to form NIs (data not shown) like any other sufficiently small mhtt fragment (Hackam et al., 1998). However, it is noteworthy that a fragment of similar size was seen after expression of another deletion mutant (aa 84–98) (data not shown), suggesting that this smaller breakdown product is most likely generated through a cleavage event in the genetically modified domain and is therefore not of relevance for this study. Nevertheless, the lack of cp-A in long-term cultured NG108 cells is consistent with the data obtained from the proteasome inhibition assay and confirms the importance of domain aa 104–114 in htt proteolysis. Finally, to determine the amino acid residues required for cleavage of cp-A, we performed an alanine-scanning mutagenesis (Figure 5A). Five T-hd122 mutants with double amino acid substitutions showed equivalent levels of mutant htt proteins in the SDS-soluble fractions, while the alanine substitutions caused a strong although differential effect on the yield of cp-A in the FA-soluble fraction (Figure 5C); substitutions NL>AA (data not shown), CL>AA, and TI>AA increased the release of cp-A, while mutants CE>AA and NI>AA caused a decrease. This set of results indicates that replacement of residues near or in the suggested cleavage site by alanine does not affect the cleavage specificity, but has an effect on the efficacy of cleavage. Similar partial effects of alanine-scanning mutagenesis were obtained by groups that studied cleavage of SREBP (Duncan et al., 1997, 1998). In concert with the result obtained with Δ104-114 htt, these data demonstrate that the amino acid modification in the aa 104–114 domain has a profound effect on the release of cp-A.

Discussion

A number of studies provide evidence that proteolytic htt fragments are sufficient to cause the HD phenotype. Htt breakdown products were identified in vitro and in brain from HD patients or in a knockin mouse model (Di Figlia et al., 1997; Wellington et al., 2000; Kim et al., 2001; Mende-Mueller et al., 2001; Wheeler et al., 2000). However, with the exception of caspase-3/6-cleaved htt fragments (Wellington et al., 2000), the htt breakdown products involved in the aggregation process have never been studied.

Heterogeneity of Nuclear and Cytoplasmic Inclusions

In this study, we focused on the identification of htt fragments present in CIs and NIs, a pathogenic hallmark in HD. We provide evidence that mutant htt fragments of different size, but shorter than the caspase fragments, differentially build up CIs and NIs. Applying immunofluorescence analysis and a disaggregation assay, we demonstrated that a fragment shorter than 115 aa, designated cp-A, and most likely its polyubiquitinated derivatives are the major mhtt-derived components present in NIs of a neuronal cell model of HD. We extended this result to the in vivo situation, as NIs identified in HD brain showed the same antigenic properties. In addition, the disaggregation of SDS-resistant material of HD brain suggests that most if not all aggregated mhtt fragments are ubiquitinated. Since ubiquitination appears after inclusion formation (Davies et al., 1997) and increases during disease progression (Gutekunst et al., 1999), it is likely to be more predominant in HD brain than in a cellular model. Our results contrast with a recent study (Dyer and McMurray, 2001) that suggests that N-terminal htt fragments observed in HD brains arise only from cleavage of wild-type htt.

CIs identified in our cellular model were heterogeneous and composed of htt fragments of different sizes: cp-A and cp-B (a htt fragment ending between aa 146–214) as well as longer processed and possibly unprocessed forms of htt, as mAb 214 and even mAb 4C8 reacted with a proportion of CIs (about 57%). It is thus possible that aggregated short forms of htt recruit the longer fragments or even full-length htt to CIs, as shown for SCA3 (Perez et al., 1998). The CIs identified in HD brain were in general built up by cp-A and contained in some instances (<10%) cp-B. In none of the CIs, the epitopes recognized by pAb 214 or by mAb 4C8 were detected under the conditions used in our study.

Cellular Compartmentalization of Htt Fragments Cp-A and Cp-B

While the presence of full-length htt in the nucleus remains controversial (Dorsman et al., 1999), very short fragments of mhtt were shown to enter the nucleus, where they accumulate (Hackam et al., 1998; Lunkes and Mandel, 1998). Given their predicted MW (less than 35 kDa for cp-B with 122 Gln), cp-A and cp-B should both be able to passively enter the nucleus. However, as only cp-A was identified to form nuclear inclusions, the subcellular sorting of cp-A and cp-B seems to depend on the domain aa 129–214. The domain present in cp-B might interact with cytoplasmic proteins, thereby preventing its import/passive diffusion into the nucleus. Alternatively, deletion of this domain in cp-A might expose the putative upstream nuclear localization signal of htt (Hackam et al., 1999), thereby allowing active nuclear import. Such an unmasking mechanism was recently demonstrated for the tumor suppressor INI1/hSNF5 (Craig et al., 2002).

Protease-Susceptible Domains in Huntingtin and Protease Specificities

In addition to caspases, calpains were proposed to cleave htt and to be involved in the formation of cytoplasmic aggregates (Kim et al., 2001). We identified the presence of several putative cleavage sites for calpain (Barrett et al., 2001) in cp-B (maximal length 214 aa). However, since the proteasome inhibitors we used also efficiently inhibit calpain I and II activities, the involvement of these proteases in the release of cp-B appears less likely.

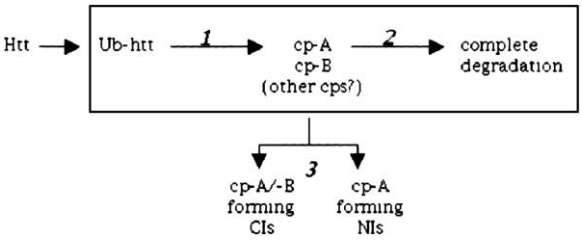

Figure 6. Normal Turnover of Mutant Htt Generates Cleavage Products with High Aggregation Potential

The model suggests that after its ubiquitination (Ub-htt), the clearance of htt proceeds through a degradation cascade (the box): htt is first proteolysed by endopeptidases (1) to release transient cleavage products (cp) which can then be degraded by the proteasomal activities (2). In the disease process, alteration of endopeptidase and/or proteasomal activities leads to intracellular accumulation of cleavage products which form either cytoplasmic or nuclear inclusions (3).

Using several approaches, we have located the cleavage site releasing cp-A in a 10 aa domain between aa 104 and 114 of htt. Notably, the use of multiple deletion mutants, not only in the in vitro proteasome inhibition assay but also in vivo in differentiated mhtt-expressing cells, showed that only deletion of aa 104–114 precluded the generation of cp-A. The finding that double amino acid substitutions covering the domain aa 104–114 did not impede the generation of cp-A in differentiated cells suggests that the protease involved has a relaxed primary sequence specificity for the cleavage site, as reported for other proteases involved in sterol signaling (Duncan et al., 1998) and Alzheimer's disease (Lichtenthaler et al., 1999; Sisodia, 1992). Since the yield of cp-A produced in NG108 cells is affected by amino acid substitutions or deletion inside or flanking the critical 10 aa domain, the recognition mechanism of the protease for its substrate appears to depend on the secondary or tertiary structure of the target domain.

A 6 hr treatment of undifferentiated cells expressing htt with proteasome inhibitors reproduced on a short time scale several molecular events which we otherwise observed in htt-expressing cells differentiated for 18 days: processing of htt, accumulation of cp-A in SDS-resistant fraction, and formation of inclusions. These similarities raise the possibility that an impairment of htt clearance is involved in the aggregation process. It is noteworthy that cp-A and cp-B were released from wild-type htt under conditions of proteasomal inhibition, indicating that the protease-susceptible domains are also readily accessible in wild-type htt before the protein enters the proteasome for degradation. Under normal culturing conditions, cp-A/cp-B, generated from both wild-type and mutant htt, were not or were faintly detectable on WBs. Most likely, they represent transient breakdown products within a degradation cascade and are immediately cleared within the cell. While accumulation

of cp-A/cp-B correlated with an inhibition of the proteasome, it is equally well conceivable that their cellular level depends, in addition, on the upstream protease activities executing their release. It is thus likely that in differentiated NG108 cells expressing mhtt, conditions leading to an increased activity of upstream proteases or an alteration of proteasomes (or both) favor the formation of polyGln aggregates (Figure 6). Since Bence et al. (2001) demonstrated that proteasomes are inhibited by aggregated polyGln proteins, one can imagine a self-amplification of this process. Given their role in the normal clearance of htt, it would be interesting to verify whether the upstream proteases are physically associated with the proteasome complex. The data obtained from the in vitro self-digestion assay suggest that the upstream proteases generating cp-A and cp-B belong to the family of pepstatin-sensitive aspartic endopeptidases, which include presenilins and the cathepsins D and E.

In conclusion, we show that protease cleavage sites in huntingtin are differentially used to release fragments building up cytoplasmic and nuclear inclusions. We suggest that aspartic proteases act in concert with the proteasome to ensure the normal clearance of htt and that during the serial proteolysis of the mutant protein, intermediate breakdown products with high aggregation potential are generated. Conditions that alter the turnover of mutant htt may provoke the accumulation of intermediate products and their aggregation. Therapeutic strategies that attenuate the production or the steady-state level of these intermediate products in neuronal cells may therefore be useful in postponing HD onset and modifying the course of manifest HD.

Experimental Procedures

Plasmids

Fl-hd116, T-hd15, T-hd73, and T-hd122 were described previously (Lunkes and Mandel, 1998). For intragene-tagged htt construct, the tetracycline-inducible vector T-hd73 was cut at the unique SacII site to introduce an HA-tag at amino acid position 82. A detailed description of hd15, hd66, hd73-101aa, hd73-124aa, and hd73-146aa as well as the deletion and mutagenesis constructs is given in the supplemental data at http://www.molecule.org/cgi/content/full/10/2/259/DC1.

Transient Transfections, Culturing, and Cell Differentiation

The culturing conditions of NG108-15 clones FL-hd116 and T-hd73 (double stable) and the activator cell line are as described before (Lunkes and Mandel, 1998) and in the supplemental data at http://www.molecule.org/cgi/content/full/10/2/259/DC1. Calcium phosphate precipitation method was used for cell transfection.

Western Blot Analysis

Whole-cell extracts were prepared for SDS-PAGE and WB analysis as described in Trottier et al. (1995a). For immunodetection, primary antibodies were diluted as follows: 1C2 and 2B4, diluted 1:1000; 1H6, diluted 1:500; 4C8, diluted 1:2000; 1259, diluted 1:200; 214, diluted 1:200. The secondary antibody (goat anti-mouse or donkey anti-rabbit immunoglobulins coupled to peroxidase) was detected using the Supersignal Substrate Western Blotting Kit (Pierce, Rockford, IL). Stripping and reprobing were performed as described in the kit manual.

Subcellular Fractionation and PolyGln Aggregates Dissociation

A three-step protocol was used to fractionate and to dissociate the polyGln aggregates. In step 1, T-hd122-expressing cells differentiated for 13 days were first fractionated to enrich for cytoplasmic and nuclear proteins, as described previously (Trottier et al., 1995b). The yields of cytoplasmic and nuclear proteins were about 90% and 10% of total cellular proteins, respectively. In step 2, cytoplasmic (2000 μg) and nuclear (300 μg) proteins were solubilized using a SDS buffer (at a final concentration of 2% SDS, 5% β-mercaptoethanol, 15% glycerol), then denatured by boiling for 10 min, and sonicated using a Vibracells sonicator (Bioblock Scientific) with a 3 mm microtip (parameters used were 20 s, 0.6:0.4 pulse on:off, amplitude 10, 4°C, to avoid foaming, aerosoling, and free radical production). SDS-soluble and SDS-resistant proteins were separated by microcentrifugation for 15 min, and the resulting pellet was washed twice with SDS buffer. In step 3, SDS-resistant material of the pellet was resuspended in 100% formic acid and incubated at 37°C for 30 min (Hazeki et al., 2000). SDS was added at 0.1% final, and then the homogenate was dried in speed-vac. The resulting dried material was finally resuspended in Laemmli loading buffer prior to WB analysis.

Proteasome Inhibition

After transient overnight transfection, NG108 cells were washed and induced for htt expression with doxicycline. 48 hr post transfection, cells were treated for 6 hr with 25 μM ALLN (Sigma), 25 μM MG132 (Calbiochem), or 10 μM lactacystin (Affinity) in DMSO. Control cells were treated equally with DMSO as carrier only or with ALLM (Sigma) in DMSO.

Self-Digestion Assay

Protein homogenates (40 μg) of undifferentiated NG108 cells expressing T-hd73 or Δ104-114 were prepared in 15 μl of cleavage buffer (50 mM PIPES/KOH [pH 6.5], 2 mM EDTA, 0.1% (w/v) CHAPS, 5 mM DTT, 1 mM PMSF) and incubated for 1 hr at 4°C or 37°C in the absence or presence of P.I.C. (aprotonin, antipain, leupeptin, chymostatin, and pepstatin, each at 2.5 μg/μl), or in the presence of the individual inhibitors (2.5 μg/μl) alone.

Human Brain Tissue

Human HD brain tissue (frontal cortex) from six individuals was obtained from the Harvard Brain Tissue Resource Center. According to the published criteria (Vonsattel et al., 1985), two cases were classified as grade 3 and four cases as grade 4 of neuropathological severity. For control, human brain tissue from three neurologically and neuropathologically normal donors was used. The post mortem interval was between 14 and 24 hr. The tissue was formalin fixed, embedded in paraffin using a standard protocol, and cut in 4 μm sections.

Acknowledgments

We would like to thank D. Helmlinger and K. Merienne for fruitful discussions; J.L. Vonesh, D. Hentsch, A. Gansmuller, and M. Oulab-Abdelghani for microscopy imaging and antibody production; Prof. J. Kirsch, Dept. of Anatomy, U. of Ulm, for granting access to a confocal laser microscope; the HBTRC, Belmont, MA (federal grant number MH/NS31862), for making HD brain tissues available to us; Prof. B. Volk and K. Müller, Dept. of Neuropathology, U. of Freiburg, for providing control brain tissues; and W. Richard, Amgen, Thousand Oaks, CA, for kindly providing pAb 214. K.S.L. was supported by the Graduiertenkolleg 460, U. of Ulm, and A.L. was supported by the Hereditary Disease Foundation, Cure Initiative (USA). This work is supported by funds from the Institut National de la Recherche Médicale (INSERM), the Centre National de Recherche Scientifique (CNRS), the Hôpital Universitaire de Strasbourg, Foundation Louis Jeantet.

Received: December 26, 2001
Revised: June 20, 2002

References

Barrett, A.J., Rawlings, N.D., and O'Brien, E.A. (2001). The MEROPS database as a protease information system. J. Struct. Biol. *134*, 95–102.

Bence, N.F., Sampat, R.M., and Kopito, R.R. (2001). Impairment of

the ubiquitin-proteasome system by protein aggregation. Science *292*, 1552–1555.

Craig, E., Zhang, Z.K., Davies, K.P., and Kalpana, G.V. (2002). A masked NES in INI1/hSNF5 mediates hCRM1-dependent nuclear export: implications for tumorigenesis. EMBO J. *21*, 31–42.

Davies, S.W., Turmaine, M., Cozens, B.A., Difiglia, M., Sharp, A.H., Ross, C.A., Scherzinger, E., Wanker, E.E., Mangiarini, L., and Bates, G.P. (1997). Formation of neuronal intranuclear inclusions underlies the neurological dysfunction in mice transgenic for the HD mutation. Cell *90*, 537–548.

Di Figlia, M., Sapp, E., Chase, K.O., Davies, S.W., Bates, G.P., Vonsattel, J.P., and Aronin, N. (1997). Aggregation of Huntingtin in neuronal intranuclear inclusions and dystrophic neurites in brain. Science *277*, 1990–1993.

Dorsman, J.C., Smoor, M.A., Maat-Schieman, M.L., Bout, M., Siesling, S., van Duinen, S.G., Verschuuren, J.J., den Dunnen, J.T., Roos, R.A., and van Ommen, G.J. (1999). Analysis of the subcellular localization of huntingtin with a set of rabbit polyclonal antibodies in cultured mammalian cells of neuronal origin: comparison with the distribution of huntingtin in Huntington's disease autopsy brain. Philos. Trans. R. Soc. Lond. B Biol. Sci. *354*, 1061–1067.

Duncan, E.A., Brown, M.S., Goldstein, J.L., and Sakai, J. (1997). Cleavage site for sterol-regulated protease localized to a leu-Ser bond in the lumenal loop of sterol regulatory element-binding protein-2. J. Biol. Chem. *272*, 12778–12785.

Duncan, E.A., Dave, U.P., Sakai, J., Goldstein, J.L., and Brown, M.S. (1998). Second-site cleavage in sterol regulatory element-binding protein occurs at transmembrane junction as determined by cysteine panning. J. Biol. Chem. *273*, 17801–17809.

Dyer, R.B., and McMurray, C.T. (2001). Mutant protein in Huntington disease is resistant to proteolysis in affected brain. Nat. Genet. *29*, 270–278.

Gutekunst, C.A., Li, S.H., Yi, H., Mulroy, J.S., Kuemmerle, S., Jones, R., Rye, D., Ferrante, R.J., Hersch, S.M., and Li, X.J. (1999). Nuclear and neuropil aggregates in Huntington's disease: relationship to neuropathology. J. Neurosci. *19*, 2522–2534.

Hackam, A.S., Singaraja, R., Wellington, C.L., Metzler, M., McCutcheon, K., Zhang, T., Kalchman, M., and Hayden, M.R. (1998). The influence of huntingtin protein size on nuclear localization and cellular toxicity. J. Cell Biol. *141*, 1097–1105.

Hackam, A.S., Singaraja, R., Zhang, T., Gan, L., and Hayden, M.R. (1999). In vitro evidence for both the nucleus and cytoplasm as subcellular sites of pathogenesis in Huntington's disease. Hum. Mol. Genet. *8*, 25–33.

Hazeki, N., Tukamoto, T., Goto, J., and Kanazawa, I. (2000). Formic acid dissolves aggregates of an N-terminal huntingtin fragment containing an expanded polyglutamine tract: applying to quantification of protein components of the aggregates. Biochem. Biophys. Res. Commun. *277*, 386–393.

Hodgson, J.G., Agopyan, N., Gutekunst, C.-A., Leavitt, B.R., LePiane, F., Singaraja, R., Smith, D.J., Bissada, N., McCutcheon, K., Nasir, J., et al. (1999). A YAC mouse model for Huntington's disease with full-length mutant huntingtin, cytoplasmic toxicity, and selective striatal neurodegeneration. Neuron *23*, 181–192.

Jana, N.R., Zemskov, E.A., Wang, G., and Nukina, N. (2001). Altered proteasomal function due to the expression of polyglutamine-expanded truncated N-terminal huntingtin induces apoptosis by caspase activation through mitochondrial cytochrome c release. Hum. Mol. Genet. *10*, 1049–1059.

Kegel, K.B., Kim, M., Sapp, E., McIntyre, C., Castano, J.G., Aronin, N., and DiFiglia, M. (2000). Huntingtin expression stimulates endosomal-lysosomal activity, endosome tubulation, and autophagy. J. Neurosci. *20*, 7268–7278.

Kim, Y.J., Yi, Y., Sapp, E., Wang, Y., Cuiffo, B., Kegel, K.B., Qin, Z.H., Aronin, N., and DiFiglia, M. (2001). Caspase 3-cleaved N-terminal fragments of wild-type and mutant huntingtin are present in normal and Huntington's disease brains, associate with membranes, and undergo calpain-dependent proteolysis. Proc. Natl. Acad. Sci. USA *98*, 12784–12789.

Klement, I.A., Skinner, P.J., Kaytor, M.D., Yi, H., Hersch, S.M., Clark, H.B., Zoghbi, H.Y., and Orr, H.T. (1998). Ataxin-1 nuclear localization and aggregation: role in polyglutamine-induced disease in SCA1 transgenic mice. Cell *95*, 41–53.

Lichtenthaler, S.F., Wang, R., Grimm, H., Uljon, S.N., Masters, C.L., and Beyreuther, K. (1999). Mechanism of the cleavage specificity of Alzheimer's disease gamma-secretase identified by phenylalanine-scanning mutagenesis of the transmembrane domain of the amyloid precursor protein. Proc. Natl. Acad. Sci. USA *96*, 3053–3058.

Lunkes, A., and Mandel, J.-L. (1998). A cellular model that recapitulates major pathogenic steps of Huntington's disease. Hum. Mol. Genet. *7*, 1355–1361.

Lunkes, A., and Mandel, J.-L. (2000). Cellular models of Huntington's disease. Neuroscience News *3*, 30–37.

Lunkes, A., Trottier, Y., Fagart, J., Schultz, P., Zeder-Lutz, G., Moras, D., and Mandel, J.-L. (1999). Properties of polyglutamine expansion in vitro and in a cellular model for Huntington's disease. Philos. Trans. R. Soc. Lond. B Biol. Sci. *354*, 1013–1019.

Mende-Mueller, L.M., Toneff, T., Hwang, S.R., Chesselet, M.F., and Hook, V.Y. (2001). Tissue-specific proteolysis of Huntingtin (htt) in human brain: evidence of enhanced levels of N- and C-terminal htt fragments in Huntington's disease striatum. J. Neurosci. *21*, 1830–1837.

Nakamura, K., Jeong, S.Y., Uchihara, T., Anno, M., Nagashima, K., Nagashima, T., Ikeda, S., Tsuji, S., and Kanazawa, I. (2001). SCA17, a novel autosomal dominant cerebellar ataxia caused by an expanded polyglutamine in TATA-binding protein. Hum. Mol. Genet. *10*, 1441–1448.

Perez, M.K., Paulson, H.L., Pendse, S.J., Saionz, S.J., Bonini, N.M., and Pittman, R.N. (1998). Recruitment and the role of nuclear localisation in polyglutamine-mediated aggregation. J. Cell Biol. *14*, 1457–1470.

Perutz, M.F., Johnson, T., Suzuki, M., and Finch, J.T. (1994). Glutamine repeats as polar zippers: their possible role in inherited neurodegenerative diseases. Proc. Natl. Acad. Sci. USA *91*, 5355–5358.

Scherzinger, E., Lurz, R., Turmaine, M., Mangiarini, L., Hollenbach, B., Hasenbank, R., Bates, G.P., Davies, S.W., Lehrach, H., and Wanker, E.E. (1997). Huntingtin-encoded polyglutamine expansions form amyloid-like protein aggregates in vitro and in vivo. Cell *90*, 549–558.

Sisodia, S.S. (1992). Beta-amyloid precursor protein cleavage by a membrane-bound protease. Proc. Natl. Acad. Sci. USA *89*, 6075–6079.

Steffan, J.S., Kazantsev, A., Spasic-Boskovic, O., Greenwald, M., Zhu, Y.Z., Gohler, H., Wanker, E.E., Bates, G.P., Housman, D.E., and Thompson, L.M. (2000). The Huntington's disease protein interacts with p53 and CREB-binding protein and represses transcription. Proc. Natl. Acad. Sci. USA *97*, 6763–6768.

Suhr, S.T., Senut, M.C., Whitelegge, J.P., Faull, K.F., Cuizon, D.B., and Gage, F.H. (2001). Identities of sequestered proteins in aggregates from cells with induced polyglutamine expression. J. Cell Biol. *153*, 283–294.

Trottier, Y., Devys, D., Imbert, G., Saudou, F., An, I., Lutz, Y., Weber, C., Agid, Y., Hirsch, E.C., and Mandel, J.L. (1995a). Cellular localization of the Huntington's disease protein and discrimination of the normal and mutated form. Nat. Genet. *10*, 104–110.

Trottier, Y., Lutz, Y., Stevanin, G., Imbert, G., Devys, D., Cancel, G., Saudou, F., Weber, C., David, G., Tora, L., et al. (1995b). Polyglutamine expansion as a pathological epitope in Huntington's disease and four dominant cerebellar ataxias. Nature *378*, 403–406.

Vonsattel, J.P., Myers R.H., Stevens, T.J., Ferrante, R.J., Bird, E.D., and Richardson, E.P., Jr. (1985). Neuropathological classification of Huntington's disease. J. Neuropathol. Exp. Neurol. *44*, 559–577.

Wellington, C.L., Singaraja, R., Ellerby, L., Savill, J., Roy, S., Leavitt, B., Cattaneo, E., Hackam, A., Sharp, A., Thornberry, N., et al. (2000). Inhibiting caspase cleavage of huntingtin reduces toxicity and aggregate formation in neuronal and nonneuronal cells. J. Biol. Chem. *275*, 19831–19838.

Wheeler, V.C., White, J.K., Gutekunst, C.A., Vrbanac, V., Weaver, M., Li, X.J., Li, S.H., Yi, H., Vonsattel, J.P., Gusella, J.F., et al. (2000). Long glutamine tracts cause nuclear localization of a novel form of huntingtin in medium spiny striatal neurons in HdhQ92 and HdhQ111 knock-in mice. Hum. Mol. Genet. *9*, 503–513.

Yamamoto, A., Lucas, J.J., and Hen, R. (2000). Reversal of neuropathology and motor dysfunction in a conditional model of Huntington's disease. Cell *101*, 57–66.

Zoghbi, H.Y., and Orr, H.T. (2000). Glutamine repeats and neurodegeneration. Annu. Rev. Neurosci. *23*, 217–247.